J. Fluid Mech. (1998), *vol.* 371, *pp.* 141–155. Printed in the United Kingdom

On the persistence of non-axisymmetric vortices in inviscid two-dimensional flows

By DAVID G. DRITSCHEL

Department of Mathematics, University of Warwick, Coventry CV4 7AL, UK

(Received 19 January 1998 and in revised form 1 May 1998)

Previous research has suggested that isolated, initially non-axisymmetric vortices in two-dimensional flows tend to become axisymmetric, in a coarse-grained sense, by purely inviscid mechanisms. That research, however, considered only vortices with broadly distributed vorticity. In this paper, it is shown that vortices with sufficiently steep edge gradients behave in a radically different way; in particular they can remain non-axisymmetric, apparently indefinitely. Such vortices, it is argued, are more typical in inviscid two-dimensional flows than the broadly distributed vortices previously considered, and hence the tendency for vortices to become axisymmetric is not generic to these flows.

1. Overview

This paper is concerned with the conditions under which an isolated vortex in a two-dimensional, inviscid flow remains indefinitely non-axisymmetric. Numerous previous works have suggested that vortices tend to become axisymmetric, in a coarse-grained sense, by cascading non-axisymmetric disturbances to ever finer scales, where they become homogeneously distributed. This cascade and homogenization both take place as a result of the differential rotation of the flow field at the periphery of the vortex.

Several counter-examples to this scenario have been reported in the literature, but no systematic study has been conducted to determine what limits the tendency for axisymmetrization. In the present work, such a systematic study is conducted using a generic class of initial vortex profiles. This class is characterized by a smoothly varying interior and an abrupt edge, at which the vorticity falls precipitously to zero. Such an abrupt edge is readily created in an inviscid fluid when a vortex is subjected to an external shear or strain flow, e.g. the flow created by another vortex some distance away.

Below, extended simulations using a novel, fast numerical algorithm indicate that vortices in this class remain persistently non-axisymmetric. However, the degree to which they remain so is shown to depend on the jump in vorticity at the edge of the vortex. In effect, sharp gradients at the edge of a vortex appear to neutralize the effect of small-scale disturbance vorticity outside the vortex. Basically, the broader the initial vortex edge, the more axisymmetric the vortex ultimately becomes. This may explain the strong tendency for axisymmetrization reported in earlier works; those works considered only broad initial vortices.

The paper is structured as follows. Section 2 reviews previous work on this problem. Section 3 describes the class of initial vortex profiles studied, briefly outlines the numerical method employed, illustrates several simulations, and summarizes, quantitatively, how the final departure from axisymmetry depends on the initial vorticity jump

at the edge of the vortex. Section 4 links the observed persistent non-axisymmetry with the existence of nearby, stable steadily rotating equilibrium vortices, and the paper concludes with a discussion of the wider applicability of the present results.

2. Background to the problem

The idea of 'axisymmetrization' (Melander, McWilliams & Zabusky 1987) grew out of an effort to explain why vortices in numerical simulations of two-dimensional turbulence often appeared to be close to circular in form (McWilliams 1984, 1990). Melander *et al.* (1987) examined in detail the numerical evolution of a single, smoothly varying, elliptically deformed vortex within a doubly periodic domain. They demonstrated that the vortex relaxes to a state close to axisymmetric on a time scale of several vortex rotations, a time scale much less than that associated with the numerical diffusion employed.

The initial stages of this process are illustrated in figure 1 for a Gaussian vortex (not the same as considered by Melander *et al.* 1987, but exhibiting qualitatively similar behaviour). The low-level vorticity is twisted around the vortex core at early times as a result of the increasing angular velocity inwards. The tongues of vorticity so created subsequently interact with the vortex core, leading to rapid axisymmetrization, or nearly so. At this stage, there is a huge mass of fine-scale vorticity surrounding the vortex core, and the subsequent evolution is sensitive to numerical diffusion. Certainly, diffusion does not help the vortex to remain non-axisymmetric.

These findings were argued to be consistent with many direct numerical simulations of two-dimensional turbulence as well as real experiments, and as such they motivated further work to understand the fundamental role played by axisymmetrization in two-dimensional vortex dynamics (see Whitaker & Turkington 1994; Yao & Zabusky 1996; Koumoutsakos 1998; Bassom & Gilbert 1998 and references therein). For example, Whitaker & Turkington (1994) have demonstrated that axisymmetric vortices are 'most-probable' equilibrium states in the statistical-mechanical theories of Miller (1990) and Robert (1991); this implies that a non-axisymmetric vortex, even an elliptical patch, will relax to an axisymmetric vortex, according to the theory, if one waits long enough. Those theories employ an ergodic mixing hypothesis to skip over the complex, inviscid evolution between the initial and final flow states, linking those states instead by a set of flow invariants (like energy, angular momentum, and the initial vorticity measure; see Turkington 1998 for background).

Recently, the behaviour of small perturbations to an axisymmetric vortex was studied analytically by Bassom & Gilbert (1998). They were able to prove that, within linear theory, such perturbations cascade to small scales and homogenize under the action of differential rotation (the inner part of the vortex rotating more rapidly than the outer part). Thus, such vortices tend to become axisymmetric. Their result further strengthens the claim of Melander *et al.* (1987) that axisymmetrization is a generic feature of vortex evolution, in the absence of external influences.

But the first indication of non-universality was suggested by an inviscid numerical simulation starting from a vortex with a steeper edge (Dritschel 1989*a*). The vortex considered began to axisymmetrize but then appeared to stabilize about a non-axisymmetric form. This form was shown to be close to a linearly stable equilibrium form. More recently, this case was re-examined by Koumoutsakos (1998), who confirmed that the vortex remains non-axisymmetric for many vortex rotation periods using an entirely different inviscid numerical algorithm.

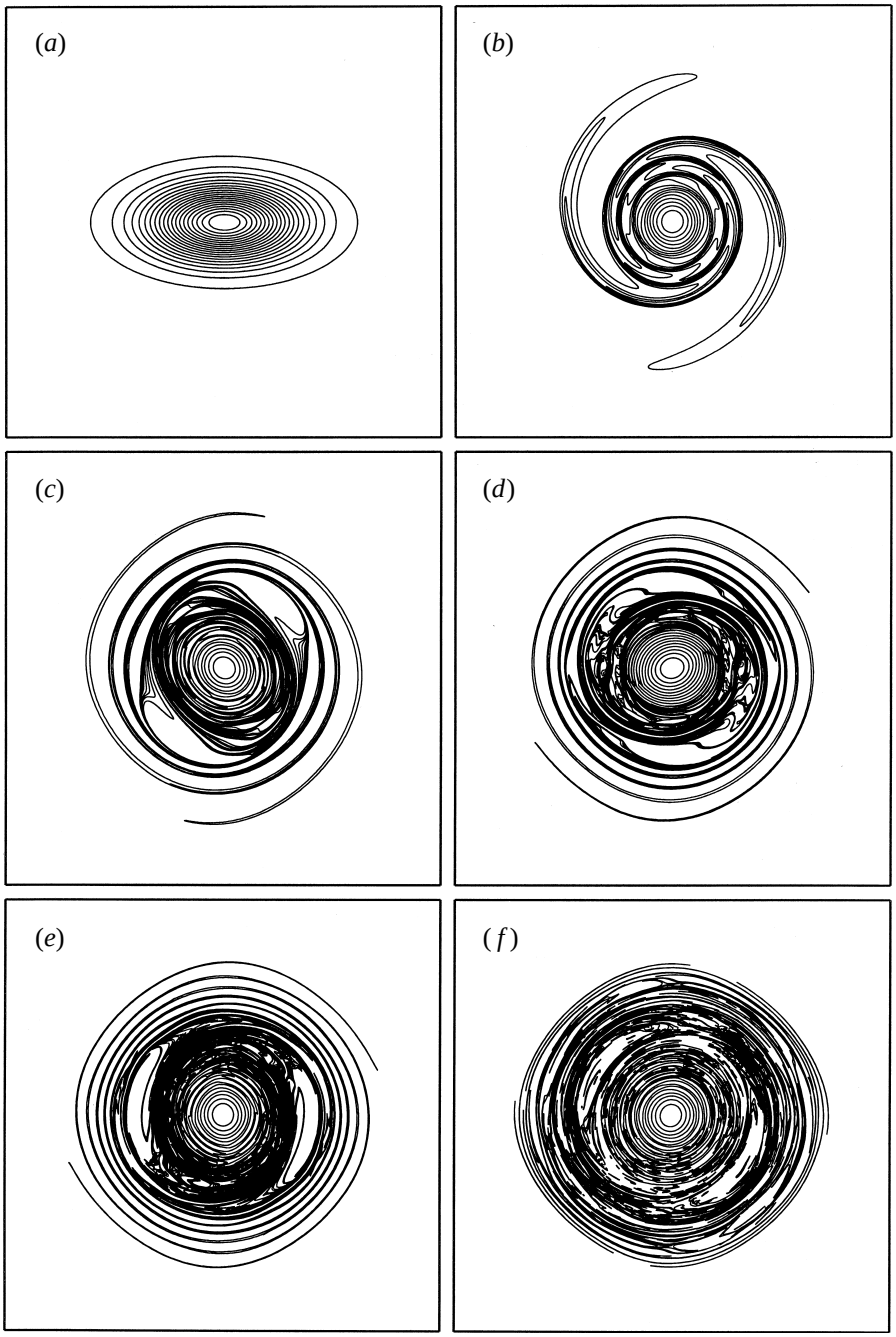

FIGURE 1. The evolution of a Gaussian vortex initially deformed into a 2:1 ellipse. The simulation is conducted at extremely high resolution using the numerical algorithm described in §3 in a doubly periodic box. A basic grid of 512^2 is used, but vorticity structures are retained down to a tenth of the grid scale. This resolution is used in all subsequent simulations except where noted. The times shown are $t = 0$, 3, 11, 18, 27 and 100 (*a–f*), in units of $T = 4\pi/\omega_{max}$. A time step of $\Delta t = 0.025$ was used in all simulations; the value of Δt is not constrained by numerical stability.

The above, however, does not contradict the findings of Bassom & Gilbert (1998), who could prove axisymmetrization only for vortices that were not 'too flat' at their centres. Specifically, the vorticity $\omega(r)$ had to behave like $1 - \alpha r^2 + O(r^4)$, with $\alpha > 0$, where r is radial distance. The profile considered in the reported exception to axisymmetrization (Dritschel 1989*a*) had $\alpha = 0$. For $\alpha = 0$, Bassom & Gilbert (1998) suggest that the differential rotation may be too weak at the vortex centre to cause axisymmetrization.

Below, a new, more serious exception is reported for a class of vortices having $\alpha > 0$. These vortices, however, are not as smooth as those considered by Bassom & Gilbert (1998), and again fall outside the scope of their analysis. Specifically, the vortices considered have a discontinuity at their edges, and we explore the degree to which non-axisymmetry persists as a function of the magnitude of this discontinuity.

One might consider this to be artificial, but it is arguably a good model for a vortex in an inviscid fluid. Fluid elements tend to stretch on average in all but the most idealized flows, and since vorticity is a materially conserved quantity, vorticity isolevels tend to stretch on average, implying, by continuity, that vorticity gradients tend to grow on average. A dramatic example of this is 'vortex stripping' (Dritschel 1989*b*; Legras & Dritschel 1993*a*,*b*), wherein low-level vorticity at the periphery of a vortex is torn away by external strain, such as that arising from a vortex further afield, leaving behind a virtual discontinuity at the vortex edge. This phenomenon is greatly affected by diffusion processes, numerical or real (Mariotti, Legras & Dritschel 1994; Yao, Dritschel & Zabusky 1995), which may explain the smooth vortex profiles seen in early simulations of two-dimensional turbulence. Without such diffusion, vortices tend to develop and maintain sharp gradients: an example is shown in figure 2 for a set of vortices starting with Gaussian vorticity profiles (the numerical algorithm employed is described in the next section). The apparent decrease in the number of vorticity isolevels by the end of the simulation is not due to diffusion; in reality, there is no decrease (since vorticity is conserved), instead the isolevels at each vortex edge have collapsed, forming virtual discontinuities.

3. Results

Following Melander *et al.* (1987) and subsequent works on axisymmetrization, we examine initially elliptical vortices, with each vorticity isolevel having the same aspect ratio $\lambda > 1$. The initial profile is defined in terms of the area $A(\omega)$ within each isolevel $\omega = \text{constant}$. In this paper, we consider the family of 'parabolic' vortices,

$$\frac{A(\omega)}{\pi} = \frac{1 - \omega/\omega_{max}}{1 - a},$$

with a discontinuity in ω at $\omega = a\omega_{max}$, where $0 \leqslant a < 1$. For an axisymmetric vortex, we would have

$$\omega(r) = \omega_{max}[1 - (1 - a)r^2]$$

for $0 \leqslant r \leqslant 1$, and $\omega(r) = 0$ otherwise. Only the case $a = 0$ is free from a discontinuity at the vortex edge. The limit $a \to 1$ corresponds to the vortex patch, and in that limit the vortex rotates steadily without change of form (Kirchhoff 1876) and is linearly stable for $\lambda < 3$ (Love 1893).

Here, we consider $\lambda = 2$, again following Melander *et al.* (1987). This is not a small deformation, and it generally leads to nonlinear behaviour, precluded from the analysis of Bassom & Gilbert (1998). As discussed in §4, the nearly circular

limit of $\lambda \to 1$ deserves closer scrutiny to understand the competing effects of small departures from axisymmetry and tight edge gradients. This competition is the key to understanding axisymmetrization.

Numerical simulations have been performed for a range of a values and numerical resolutions. The simulations have been conducted with the new 'Contour-Advective Semi-Lagrangian' (CASL) algorithm (Dritschel & Ambaum 1997), which combines the most efficient and accurate parts of the Lagrangian contour dynamics/surgery method (Dritschel 1989*a*) and the Eulerian pseudo-spectral method (Gottlieb & Orszag 1977). The CASL algorithm represents the vorticity as material contours, which are advected by the velocity field interpolated from an underlying grid. That velocity field is obtained using the standard machinery of a pseudo-spectral method, i.e. FFTs, spectral inversion of $\nabla^2\psi = \omega$ for the streamfunction ψ, spectral calculation of the velocity field $u = -\partial\psi/\partial y$, $v = \partial\psi/\partial x$, and inverse FFTs to get u and v on the grid. The advection of vorticity contours corresponds to solving $\mathrm{D}\omega/\mathrm{D}t = 0$. This contour advection avoids the need for numerical diffusion to maintain stability, frees one from the CFL constraint on the time step, and permits a much finer, more accurate representation of the vorticity. In the CASL algorithm, vorticity features are retained below grid scale, and dissipation occurs only to filamentary vorticity at a tenth of the grid scale – sharp gradients are never smeared out. This results in a dramatic improvement in solution accuracy compared to conventional methods and a great savings in computer time; this is demonstrated in Dritschel & Ambaum (1997) and Dritschel, Polvani & Mohebalhojeh (1998*a*).

The contour representation implies that the vorticity is formally piecewise-constant, that is, the vorticity jumps across each contour. In practice, however, the contours must be momentarily converted to gridded values for use in obtaining the velocity field, and this implies that the vorticity discontinuities are rounded off at the grid scale. It turns out though that this fine-scale vorticity contributes negligibly to the advecting velocity field (Dritschel & Ambaum 1997). The bottom line is that it is accurate to represent smooth vorticity distributions in this way (see Legras & Dritschel 1993*b*; DiBattista & Polvani 1998; and Dritschel *et al.* 1998*a*).

In the simulations below, the vorticity profile is discretized into n steps, with $n = 20$ used most often. Equal jumps in vorticity $\Delta\omega$ are used at each contour except for the outer edge; the discretization ensures that at each contour the discretized vortex has the same circulation as the continuous vortex. Specifically, the area of contour j is given by $A_j = j\pi/n$, $j = 1, \ldots, n$, and the vorticity jumps are $\Delta\omega = (1-a)\omega_{max}/n$ except at the outer edge, where the jump is equal to $a\omega_{max} + \Delta\omega/2$. Most of the simulations have been conducted using a 512^2 grid, and in all cases, dissipation of filamentary structures by 'surgery' (Dritschel 1989*a*) takes place at one tenth of the grid scale. This resolution is shown to be adequate below. Without loss of generality, we take $\omega_{max} = 4\pi$, so that time $t = 1$ corresponds to the rotation period of a fluid element at the centre of an axisymmetric vortex. The time step is chosen to be $\Delta t = 0.025$; the results are not sensitive to Δt for values smaller than this. Each contour is represented by a variable number of points (connected by local cubic splines), whose local density is proportional to the square root of local curvature. The dimensionless node separation parameter $\mu = (0.4\Delta x)^{1/2}$, where Δx is the grid scale, and the box has dimensions $2\pi \times 2\pi$ (the mean radius of the vortex is 1). For the conversion of the vorticity contours to gridded values, a grid twice as fine is used, with 9-point averaging to produce vorticity values on the original grid (see Dritschel & Ambaum 1997 for full details of these standard parameter settings).

(*a*)

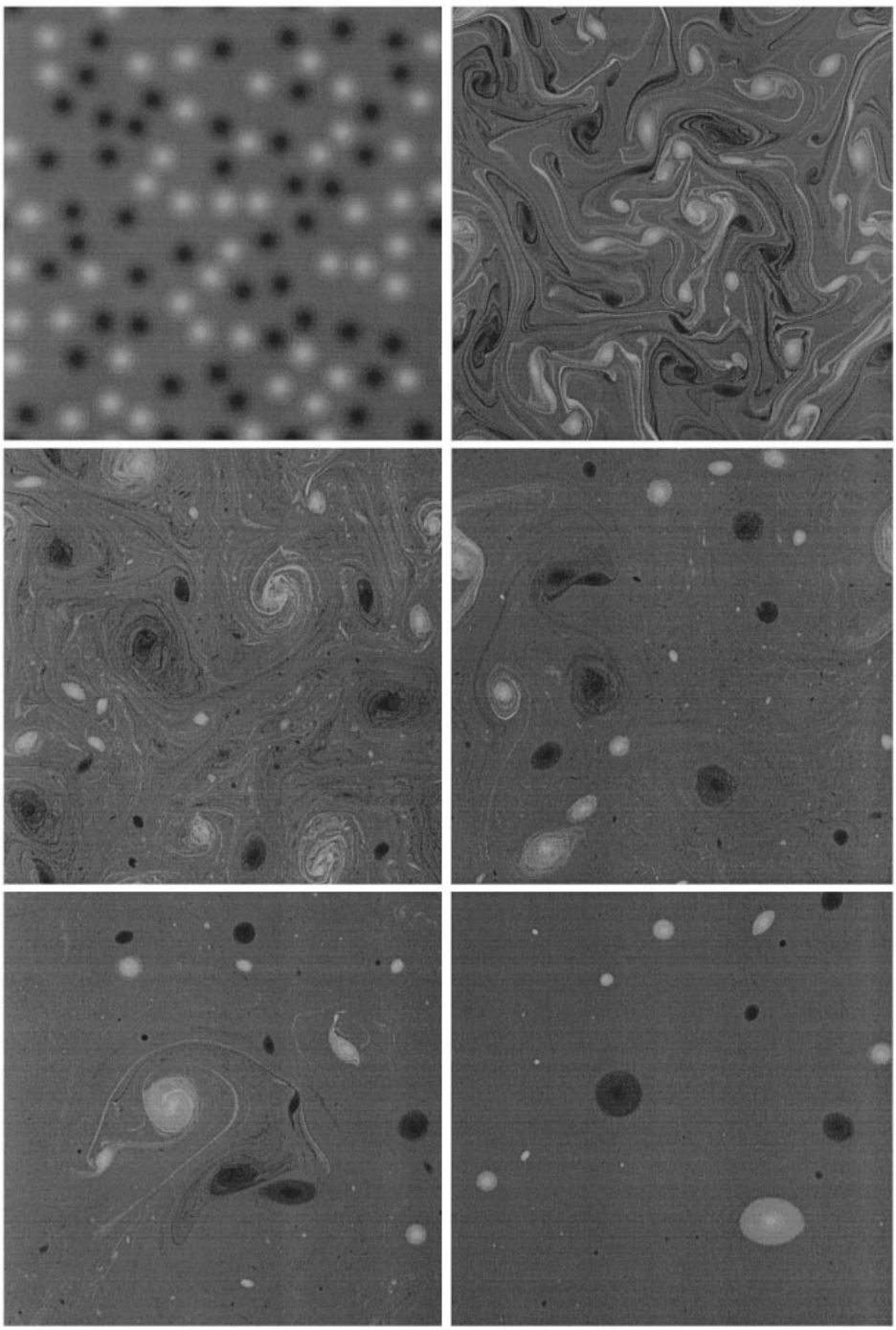

FIGURE 2. (*a*) For caption see facing page.

(*b*)

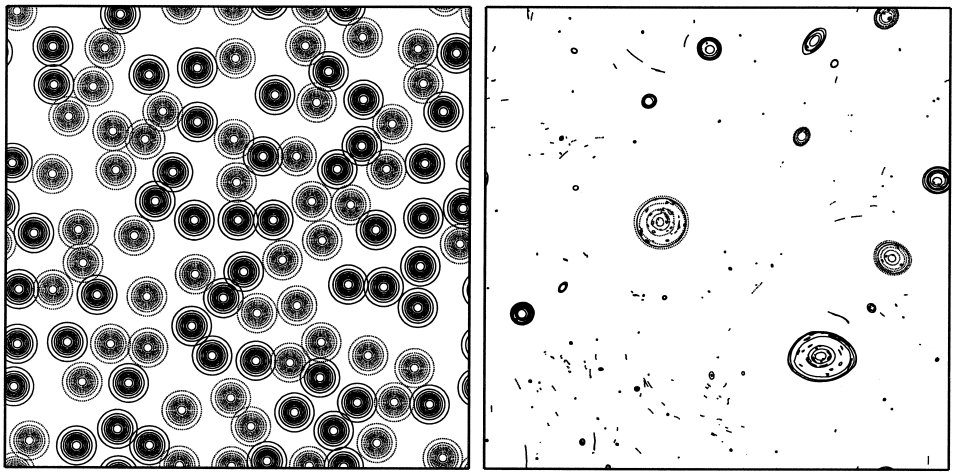

FIGURE 2. (*b*) The evolution of a set of initially Gaussian vortices in a doubly periodic box. All of the vortices are identical, except half have positive vorticity and half have negative vorticity. (*a*) The evolution in grey-scale form, at times $t = 0$, 4, 12, 24, 38 and 200, in units of $T = 4\pi/|\omega|_{max}$. (*b*) The initial and final times in contour form. Eight contours are used to represent each vortex initially (see left panel, which shows the actual contours (which overlap in places), not the field isolevels); the apparent decrease in the number of contours by the end of the simulation is due to the stripping of low-level vorticity. The resultant jump in vorticity at the edge of each vortex ranges between a third and two thirds of $|\omega|_{max}$ for nearly all vortices.

Figure 3 shows the vorticity contours at $t = 2$, 8, 20 and 100 from three simulations, (*a*) for $a = 0$, (*b*) for $a = 0.2$ and (*c*) for $a = 0.4$. As a increases, the discontinuity at the vortex edge increases, and this enables the vortex to better resist axisymmetrization. In all three cases, the vortex equilibrates about a non-axisymmetric form (quantified below). Even when $a = 0$, the vortex edge is steep enough to avoid complete axisymmetrization (contrast this with the initially Gaussian vortex in figure 1). In all cases, the initial evolution is qualitatively similar: the outer tips of the vortex rotate more slowly than the inner core, creating encircling tongues of vorticity. These tongues carry less and less circulation for increasing a, even though they contain higher amplitude vorticity. For $a \gtrsim 0.6$, no tongues at all are produced – see figure 4 for $a = 0.6$. This is because the vortex is then close to a rotating equilibrium form (these have been computed and have been found to be linearly stable, see §4 below), and the disturbances to this equilibrium are too small to be convected away. Basically, the equilibrium vortex is surrounded by a small zone of trapped fluid, bounded externally by a separatrix. The separatrix consists of closed curves that intersect at critical points, i.e. points where the velocity vanishes in the frame rotating with the equilibrium vortex. If the disturbance to the equilibrium form is too large, fluid can escape from the trapped zone around the vortex, which is what is happening in the simulations shown in figure 3 at early times.

The subsequent evolution for $a < 0.6$, not shown in detail, consists of the repeated interaction of the vorticity tongues with the vortex core. This leads to partial axisymmetrization. Each interaction leaves the external disturbance vorticity more spread out and at finer scale, so that each subsequent interaction affects the vortex core progressively less. In these cases, the straining field induced by the vortex core efficiently stretches and scrambles the disturbance vorticity, rendering it practically

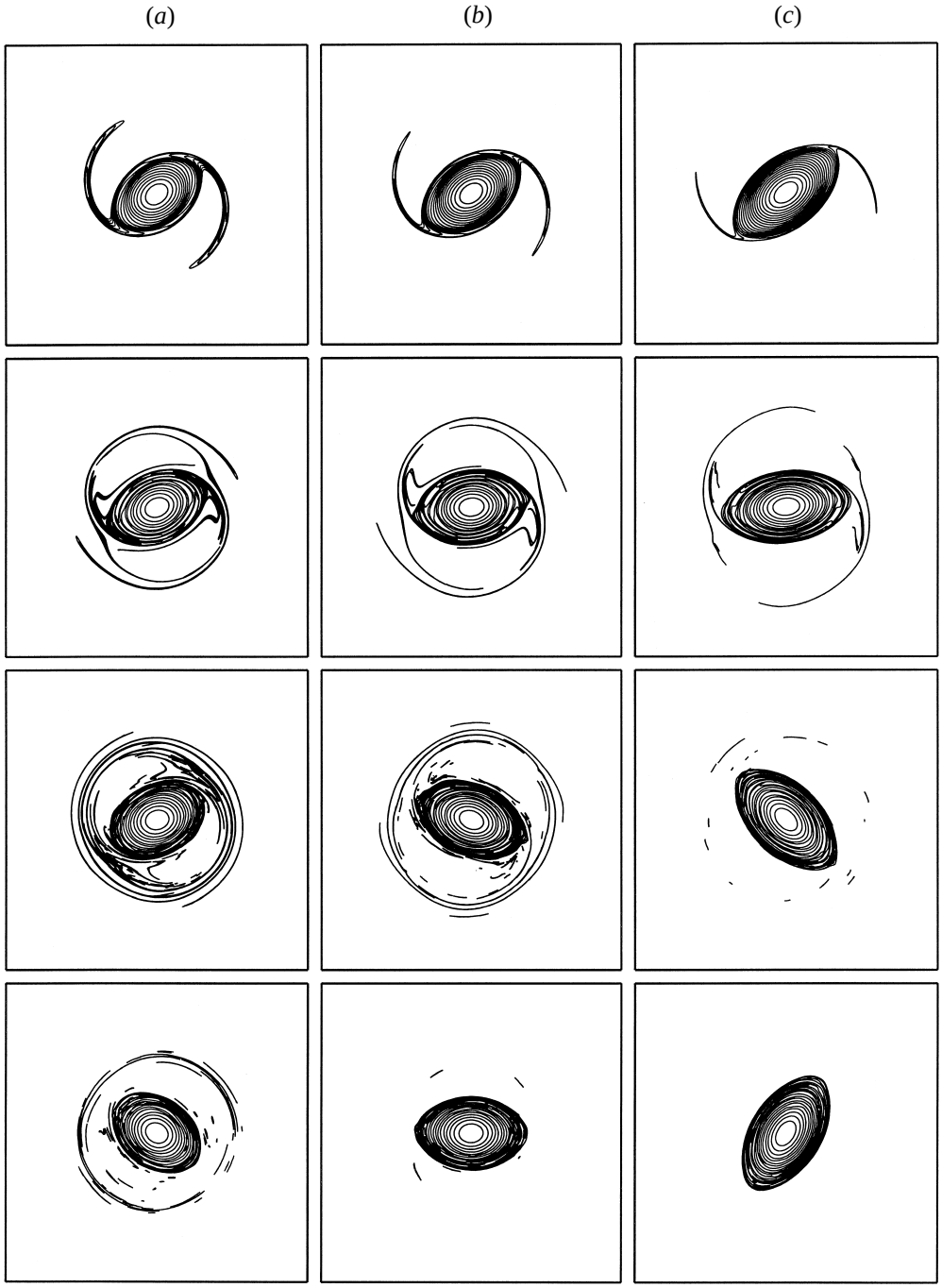

FIGURE 3. The evolution of three different initial vortices: (*a*) for $a = 0$, (*b*) for $a = 0.2$ and (*c*) for $a = 0.4$. Time proceeds downwards; the times shown are $t = 2$, 8, 20 and 100.

passive (note, the disturbance vorticity is not removed until it has reached a tenth of the grid scale, i.e. about a thousandth of the vortex radius, a scale which is far smaller than in any previous simulation of this process; higher resolution is considered immediately below).

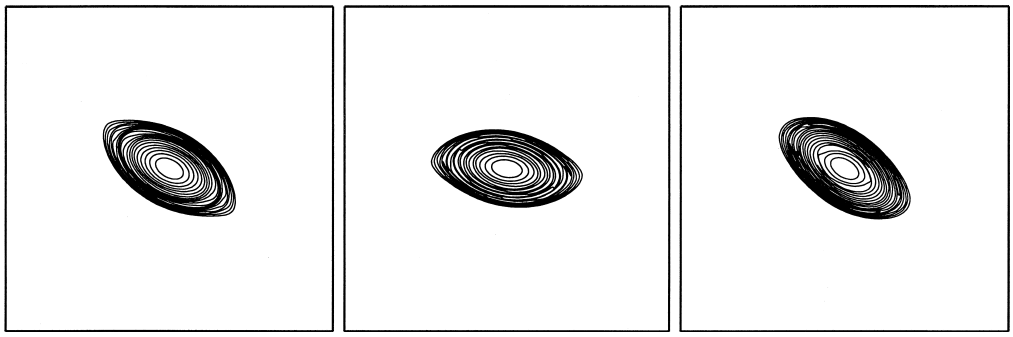

FIGURE 4. The evolution of an initial vortex with $a = 0.6$. Time proceeds from left to right ($t = 9$, 20 and 100 are shown). The differential rotation of the vortex here causes initial disturbances to the underlying equilibrium to break internally; this breaking however has only a minor effect on the gross properties of the vortex. With increasing edge vorticity jump, vortices display progressively less internal wave-breaking.

n_g	$\bar{\lambda}$
64	1.265
128	1.290
256	1.299
512	1.299
1024	1.284

TABLE 1. Dependence of $\bar{\lambda}$ on the grid resolution n_g. *Note:* These results were obtained for the case $a = 0$, with $n = 20$ contours. The small, unsystematic variations in $\bar{\lambda}$ are principally due to uncontrollable differences that develop after long times in systems that are inherently unpredictable.

The degree of axisymmetrization is quantified by computing the mean aspect ratio of the vortex core, defined here as the vorticity $\omega > (1 + a)\omega_{max}/2$, a value midway between the peak and edge values. That aspect ratio λ_c is computed as in Melander *et al.* (1987) and Dritschel (1989*a*) using the expression

$$\lambda_c = \left(\frac{J + R}{J - R}\right)^{1/2}$$

where $J = J_{20} + J_{02}$, $R = [(J_{20} - J_{02})^2 + 4J_{11}^2]^{1/2}$, and $J_{mn} = \iint x^m y^n \omega(x, y) \mathrm{d}x\mathrm{d}y$, restricted as above.

Figure 5 shows first the evolution of λ_c for the case $a = 0$ (no discontinuity at the vortex edge); three curves are drawn, corresponding to variations in the numerical resolution. The bold line shows the results obtained using $n = 20$ contours and a basic grid of 512^2 (the simulation shown in figure 3*a*), the dashed line shows the effect of doubling n, while the thin solid line shows the effect of halving the grid size (and thus the dissipation scale). These variations affect only the details of the evolution; the time-mean values of λ_c over the last 10 units of time are $\bar{\lambda} = 1.299$, 1.296, and 1.284, respectively. Moreover, results for a 16-fold range in grid sizes are given in table 1 to emphasize that the value of $\bar{\lambda}$ is not sensitive to numerical resolution, i.e. to the presence or not of thin filamentary structures surrounding the vortex.

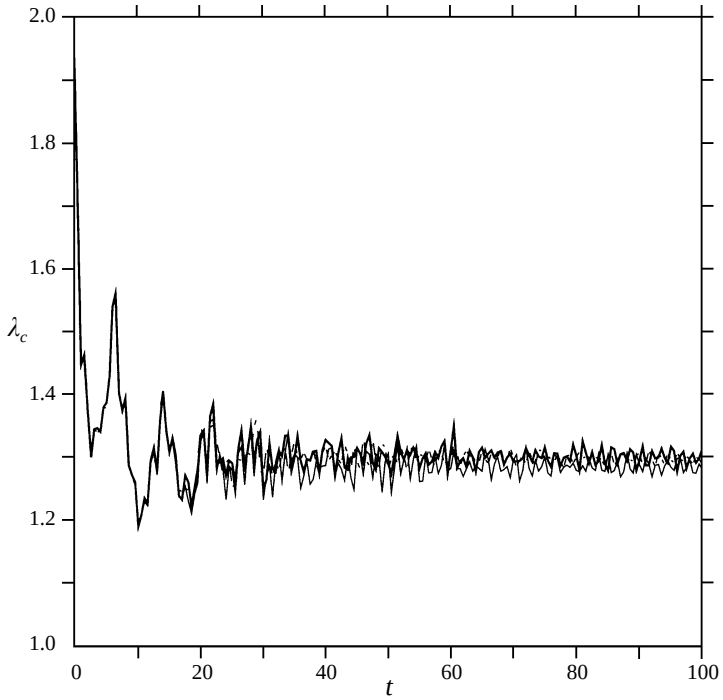

FIGURE 5. The evolution of λ_c for the case $a = 0$ and for different numerical resolutions. The bold line is for $n = 20$ contours and a 512^2 grid, the thin line is for twice as many contours, and the dashed line is for twice as many grid points in each direction.

Figure 6 compares the evolution of λ_c for several vortices, $a = 0.8$ (top), $a = 0.4$ and $a = 0$ (middle), and the Gaussian vortex in figure 1 (bottom). The case $a = 0.8$ does not exhibit wave-breaking, externally or internally, but the aspect ratio displays strong, nearly regular oscillations, no doubt related to the linear wave dynamics on the underlying equilibrium vortex. The other cases exhibit complex behaviour, precipitated by the initial ejection of tongues of vorticity; nonetheless, they all apparently settle down to a near-equilibrium vortex with small oscillations. The aspect ratio of the Gaussian vortex reaches unity several times (when the semi-major and semi-minor axes exchange); in a time mean, the vortex is indistinguishable from a circular vortex. It is expected that the small remaining disturbances in this case will decay away according to the linear analysis of Bassom & Gilbert (1998).

The principal result of this paper is shown in figure 7, which shows how the late time-mean aspect ratio $\bar{\lambda}$ varies with the dimensionless jump in vorticity at the vortex edge a. When $a = 1$, the vortex is an elliptical patch, and $\bar{\lambda}$ remains unchanged at 2. As a decreases, so does $\bar{\lambda}$, because more disturbance vorticity is available to interact with the vortex core. However, even at $a = 0$, $\bar{\lambda}$ remains significantly greater than 1. The vorticity profile is still steep enough to resist complete axisymmetrization.

4. Discussion

The steepness of the vortex edge is seen to control the extent to which a vortex axisymmetrizes. This factor was overlooked in many previous studies of this process, most probably because early numerical simulations suggested that vortices in two-

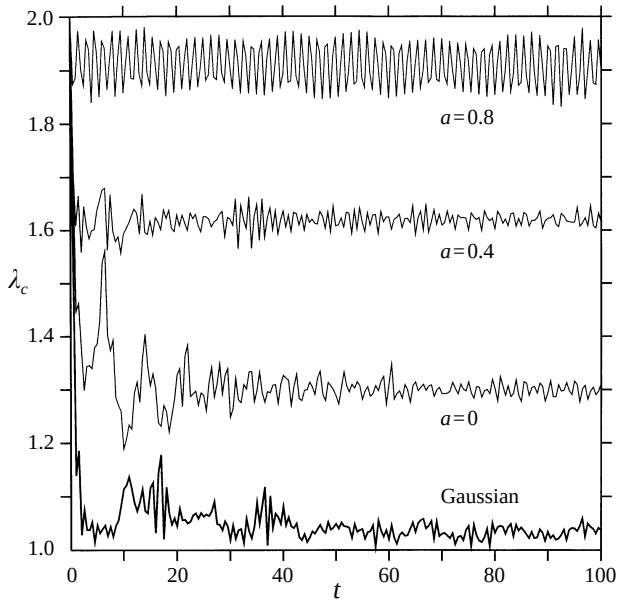

FIGURE 6. The evolution of λ_c for several initial vortices; from top to bottom, the curves correspond to $a = 0.8$, $a = 0.4$, $a = 0$, and the Gaussian vortex in figure 1 (distinguished also by a bold line).

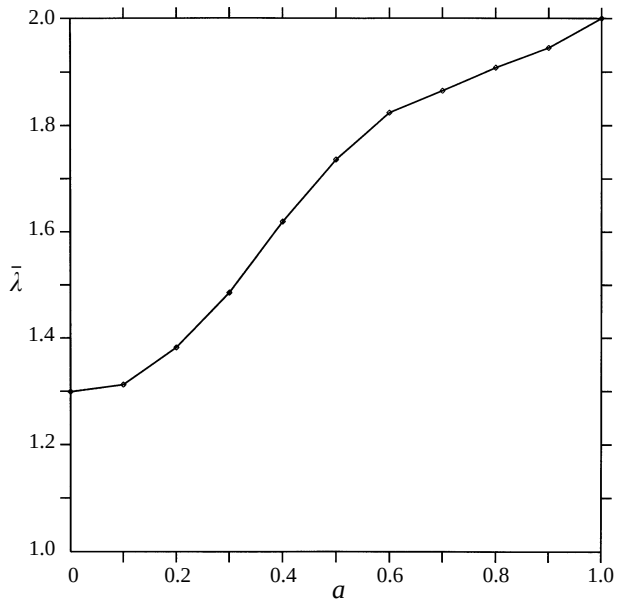

FIGURE 7. The average of λ_c over the time interval $[90, 100]$ for simulations conducted with $a = 0$, 0.1, 0.2, ..., 0.9. Also shown is the trivial result for $a = 1$, an elliptical patch, which preserves its aspect ratio.

dimensional turbulence tend to have broad profiles (cf. figure 11 from McWilliams 1990). The role of numerical diffusion in creating this picture, however, was underestimated (see remarks in Dritschel 1993; Mariotti *et al.* 1994; and Yao *et al.* 1995). The image shown in figure 2, for inviscid two-dimensional turbulence, is strikingly

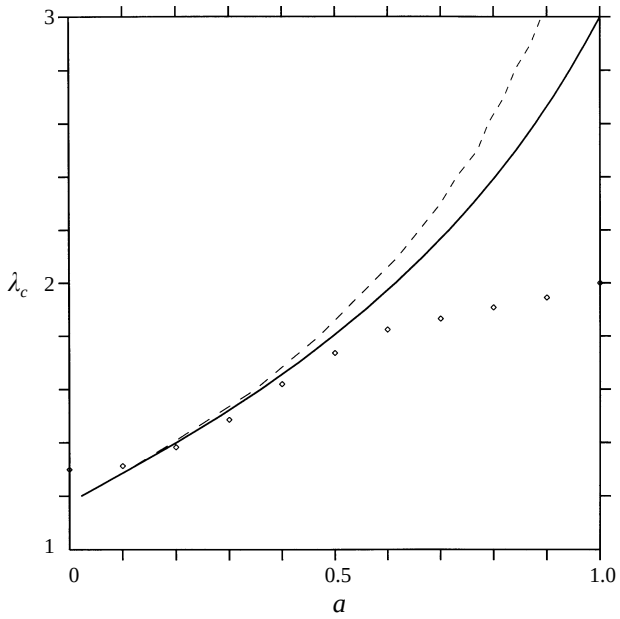

FIGURE 8. Regime diagram for steadily rotating parabolic vortices with a discontinuity at $\omega = a\omega_{max}$. The equilibria are found by prescribing the core aspect ratio λ_c (as defined in the text). The numerical procedure is described in Dritschel (1995). Equilibria can be found below and to the right of the dashed curve (corresponding approximately to the limiting equilibria having corners (and therefore critical points) on their outer boundaries). Linearly stable equilibria can be found below and to the right of the bold curve. The stability has been calculated as described in Dritschel (1995); the marginal stability curve is accurate to within the plotted line width. The diamonds are the points from figure 7, i.e. the late-time mean λ_c values for each simulation conducted.

different from the images generated by conventional numerical simulation methods, yet it is the natural consequence of kinematic stretching, without diffusion, in these flows. One can conclude from such an image that broad vorticity profiles are distinctly unnatural, and hence, from the present work, that vortices in general do not axisymmetrize.

The persistence of non-axisymmetry appears to be intimately connected with the existence of underlying, nearby, stable equilibrium vortices. Dritschel (1989*a*) and Dritschel & Legras (1991) have computed such vortices and have determined their linear stability. They found stable equilibrium vortices only for sufficiently steep edge gradients, depending on the departure from axisymmetry. The greater this departure, the steeper the edge has to be. For the class of vortices examined in the present work, the domain of (linearly) stable equilibria in the (a, λ_c)-plane is shown in figure 8 (below and to the right of the bold curve). Also plotted in figure 8 are the data points from figure 7 – note that they all lie in the stable regime, except when $a \leqslant 0.1$ (for reasons given below). The idea here is that the numerically simulated vortices equilibrate around one of the stable equilibria. This is made more convincing by figure 9, which compares several of the simulated and equilibrium vortices having the same a and λ_c values. The comparison is all the more remarkable when one realizes that the vortices compared do not have exactly the same area between vorticity contours (some area near the outer edge has been lost by the simulated vortices); this is particularly true for small values of a and explains why the data points for $a = 0$ and $a = 0.1$ in figure 8 are shifted too far to the left (the appropriate equilibrium vortex would have

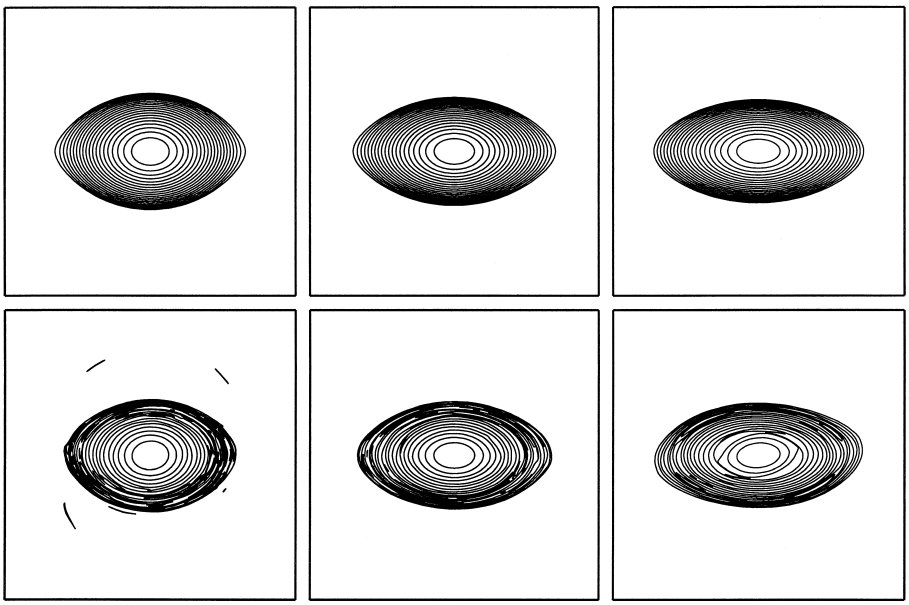

FIGURE 9. Comparison of the steadily-rotating equilibria (top row) with the corresponding simulated vortices (bottom row) for $a = 0.2$, 0.4 and 0.6 (left to right). The vortices have the same aspect ratios (the late-time mean aspect ratio of the simulated vortices is used to make the association).

a bigger value of a, i.e. a bigger vorticity jump at its edge). If this were corrected for, e.g. by finding equilibria with the same area between contours as the simulated vortices, the comparison would be even better. The upshot is that vortices can evolve into stable, non-axisymmetric vortices, which may therefore persist indefinitely.

The limiting case of a nearly axisymmetric vortex, considered by Bassom & Gilbert (1998) is more subtle, and deserves closer scrutiny. First of all, almost all perturbations from an axisymmetric state lead to unsteady behaviour. Though there may be an underlying equilibrium, the disturbances to this equilibrium may be of comparable amplitude; this appears to be true for almost all perturbations. In this case, like the Gaussian vortex considered in figure 1, enough disturbance vorticity is present to enable axisymmetrization to take place. However, if one were to first determine a slightly non-axisymmetric equilibrium, and then introduce disturbances of much smaller amplitude, one might find that axisymmetrization does not take place. Not all vorticity profiles admit equilibria; one must ensure that, in the frame of reference rotating with the vortex, the (hyperbolic) critical points where the velocity field vanishes lie completely outside the vortex – this is most easy to ensure for a compact, steep-edged vortex. It appears that this problem is analytically tractable using the techniques developed by Bassom & Gilbert (1998).

Although it is not possible to claim, definitively, that a generic class of vortices may never axisymmetrize on the basis of numerical simulation alone, the present results at least indicate that axisymmetrization as predicted by the statistical theory (cf. Whitaker & Turkington 1994) can only occur on extraordinarily long time scales. In geophysical fluid dynamics, a main application area for research on two-dimensional vortex dynamics, vortex isolation over such time scales never occurs, and thus slow, statistical axisymmetrization (if it takes place at all) is not relevant. The statistical 'theory' is itself not definitive on this point, since the ergodic mixing hypothesis on

which it is based remains unproved (and questionable – see e.g. Sommeria, Staquet & Robert 1991; Chen & Cross 1996; and Brands 1998).

Finally, the persistence of non-axisymmetric vortices can be expected in more general, three-dimensional, rotating, stably stratified flows (e.g. the Earth's atmosphere and oceans). The two-dimensional flow considered in this paper is the lowest-order approximation to the true three-dimensional flow (and sometimes a misleading one, see Dritschel, de la Torre Juárez & Ambaum 1998*b*), but it shares a number of common features, including a materially conserved advected quantity (potential vorticity) and purely horizontal motion (motion parallel to stratification surfaces). In both flows, horizontal straining generates sharp gradients at the edges of vortices, and hence vortices in three-dimensional rotating, stably stratified flows may resist axisymmetrization for the same reasons their two-dimensional counterparts do.

In summary, sharp vorticity gradients are generic to inviscid flows. These gradients both protect vortices from external influences and enable non-axisymmetric deformations to persist for long times, perhaps indefinitely. Diffusion processes, by reducing edge gradients, make a vortex more susceptible to axisymmetrization, which may explain why nearly-axisymmetric vortices had been observed so frequently in early numerical simulations and experiments of two-dimensional flows.

Support for this research has come from the UK Natural Environment Research Council.

REFERENCES

Bassom, A. P. & Gilbert, A. D. 1998 The spiral wind-up of vorticity in an inviscid planar vortex. *J. Fluid Mech.* **371** 109–140.

Brands, H. 1998 PhD Thesis, University of Amsterdam (in preparation).

Chen, P. & Cross, M. C. 1996 Mixing and thermal equilibrium in the dynamical relaxation of a vortex ring. *Phys. Rev. Lett.* **77**, 4174–4177.

DiBattista, M. T. & Polvani, L. M. 1998 Barotropic vortex pairs on a rotating sphere. *J. Fluid Mech.* **358**, 107–133.

Dritschel, D. G. 1989*a* Contour dynamics and contour surgery: numerical algorithms for extended, high-resolution modelling of vortex dynamics in two-dimensional, inviscid, incompressible flows. *Comput. Phys. Rep.* **10**, 77–146.

Dritschel, D. G. 1989*b* Strain-induced vortex stripping. In *Mathematical Aspects of Vortex Dynamics* (ed. R. E. Caflisch), pp. 107–119, SIAM.

Dritschel, D. G. 1993 Vortex properties of two-dimensional turbulence. *Phys. Fluids* A **5**, 984–997.

Dritschel, D. G. 1995 A general theory for two-dimensional vortex interactions. *J. Fluid Mech.* **293**, 269–303.

Dritschel, D. G. & Ambaum, M. H. P. 1997 A contour-advective semi-Lagrangian algorithm for the simulation of fine-scale conservative fields. *Q. J. R. Met. Soc.* **123**, 1097–1130.

Dritschel, D. G. & Legras, B. 1991 The elliptical model of two-dimensional vortex dynamics. Part II: disturbance equations. *Phys. Fluids* A **3**, 855–868.

Dritschel, D. G., Polvani, L. M. & Mohebalhojeh, A. R. 1998*a* The contour-advective semi-Lagrangian algorithm for the shallow water equations. *Mon. Wea. Rev.* (in press).

Dritschel, D. G., Torre Juárez, M. de la & Ambaum, M. H. P. 1998*b* The three-dimensional vortical nature of atmospheric and oceanic turbulent flows. *Phys. Fluids* (submitted).

Gottlieb, D. & Orszag, S. A. 1977 *Numerical Analysis of Spectral Methods: Theory and Applications.* SIAM.

Kirchhoff, G. 1876 *Vorlesungen über mathematische Physik.* Leipzig: Mechanik.

Koumoutsakos, P. 1998 Inviscid axisymmetrization of an elliptical vortex. *J. Comput. Phys.* **138**, 821–857.

Legras, B. & Dritschel, D. G. 1993*a* Vortex stripping and the generation of high vorticity gradients in two-dimensional flows. *Appl. Sci. Res.* **51**, 445–455.

LEGRAS, B. & DRITSCHEL, D. G. 1993*b* A comparison of the contour surgery and pseudo-spectral methods. *J. Comput. Phys.* **104**, 287–302.

LOVE, A. E. H. 1893 On the stability of certain vortex motions. *Proc. Lond. Math. Soc.* **35**, 18.

MARIOTTI, A., LEGRAS, B. & DRITSCHEL, D. G. 1994 Vortex stripping and the erosion of coherent structures in two-dimensional flows. *Phys. Fluids* **6**, 3954–3962.

MCWILLIAMS, J. C. 1984 The emergence of isolated coherent vortices in turbulent flow. *J. Fluid Mech.* **146**, 21–43.

MCWILLIAMS, J. C. 1990 The vortices of two-dimensional turbulence. *J. Fluid Mech.* **219**, 361–385.

MELANDER, M. V., MCWILLIAMS, J. C. & ZABUSKY, N. J. 1987 Axisymmetrization and vorticity-gradient intensification of an isolated two-dimensional vortex through filamentation. *J. Fluid Mech.* **178**, 137–159.

MILLER, J. 1990 Statistical mechanics of Euler equations in two dimensions. *Phys. Rev. Lett.* **65**, 2137–2140.

ROBERT, R. 1991 A maximum-entropy principle for two-dimensional perfect fluid dynamics. *J. Statist. Phys.* **65**, 531–553.

SOMMERIA, J., STAQUET, C. & ROBERT, R. 1991 Final equilibrium state of a two dimensional shear layer. *J. Fluid Mech.* **233**, 661–689.

TURKINGTON, B. 1998 Statistical equilibrium measures and coherent states in two-dimensional turbulence. *Comm. Pure Appl. Math.* (submitted).

WHITAKER, N. & TURKINGTON, B. 1994 Maximum entropy states for rotating vortex patches. *Phys. Fluids* **6**, 3963–3973.

YAO, H. B., DRITSCHEL, D. G. & ZABUSKY, N. J. 1995 High-gradient phenomena in 2D vortex interactions. *Phys. Fluids* **7**, 539–548.

YAO, H. B. & ZABUSKY, N. J. 1996 Axisymmetrization of an isolated vortex region by splitting and partial merging of satellite depletion perturbations. *Phys. Fluids* **8**, 1842–1847.